

## Large-area microlens emitters for powerful THz emission

G. Matthäus · S. Nolte · R. Hohmuth · M. Voitsch ·  
W. Richter · B. Pradarutti · S. Riehemann · G. Notni ·  
A. Tünnermann

Received: 6 March 2009 / Revised version: 20 May 2009 / Published online: 18 June 2009  
© Springer-Verlag 2009

**Abstract** A microlens coupled large-area emitter based on low-temperature grown GaAs is presented. A hexagonal microlens array directs the incident pump light into every second gap of a finger electrode structure. Consequently, an unidirectional photocurrent at high acceleration field strengths (50 kV/cm) is achieved, which generates constructively superposed THz emission. Using a Ti:Sapphire oscillator with a maximum average power of about 3 W at a repetition rate of 80 MHz, a net IR-to-THz conversion efficiency up to  $1.3 \times 10^{-4}$  and a THz average power of 280  $\mu\text{W}$  is achieved.

**PACS** 42.65.Re · 95.85.Gn · 85.60.-q

### 1 Introduction

Today, the generation of picosecond electromagnetic pulses in the frequency range of 100 GHz to above 10 THz using ultrashort near infrared pulses is a well-established technique. Driven by scientific and industrial applications such as spectroscopy, tomography, quality assurance, or homeland secu-

rity, basically two major generation types have been developed. Depending on the pump laser characteristics, either optical rectification or ultrafast photocurrents are the preferred mechanisms. Generally, for amplified laser systems working at or below kHz repetition rates, nonlinear effects would be the favored method since nonlinear optical crystals have significant higher optical damage thresholds than semiconductors like GaAs or InGaAs. However, for compact high average power lasers running at MHz repetition rates, photoconductive switches (PC switch) are commonly used due to their superior THz-to-IR conversion efficiencies at around  $10^{-5}$ – $10^{-4}$  [1, 2]. In particular, for environmental stable and portable THz systems, high-repetition rate lasers in combination with PC switches are mostly preferred.

Over recent years, several different attempts have been made in order to optimize the THz efficiency and output power, respectively [3–8]. Especially, tomographic applications and spatial resolved spectroscopy require extraordinary rapid THz pulse sampling which can be realized with an increased THz output in order to accelerate the data acquisition while a sufficient high signal-to-noise ratio can be preserved [9, 10]. However, still today, phase-sensitive THz measurements of extended objects generally require several minutes, hours, or even days, depending on the size of the object and the intended spectral or spatial resolution.

We recently reported on a microlens-coupled interdigital photoconductive switch as high-efficient THz emitter with an active area of approximately  $300 \times 300 \mu\text{m}^2$  [2]. This device is based on a hexagonal microlens array which is attached to a finger electrode structure processed on low-temperature grown GaAs (LT GaAs). The microlenses direct the incident pump light onto the PC switch in such a way that only every second electrode gap is illuminated. As a consequence, a unidirectional photocurrent is induced,

G. Matthäus (✉) · S. Nolte · A. Tünnermann  
Institute of Applied Physics, Friedrich-Schiller-University Jena,  
Max-Wien-Platz 1, Jena 07743, Germany  
e-mail: [gabor.matthaeus@uni-jena.de](mailto:gabor.matthaeus@uni-jena.de)  
Fax: +49-(0)3641-947802

R. Hohmuth · M. Voitsch · W. Richter  
BATOP GmbH, Wildenbruchstrasse 15, Jena 07745, Germany

S. Nolte · B. Pradarutti · S. Riehemann · G. Notni ·  
A. Tünnermann  
Fraunhofer Institute for Applied Optics and Precision  
Engineering, Albert-Einstein-Strasse 7, Jena 07745, Germany

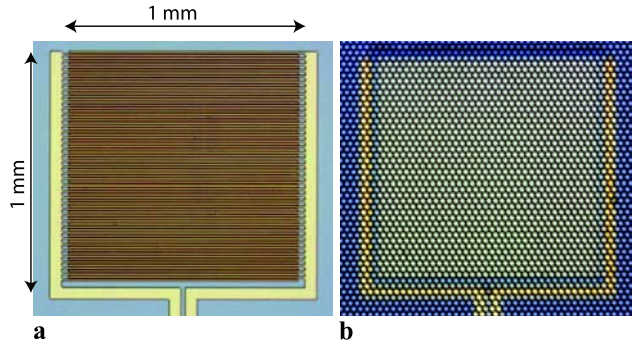


**Fig. 1** Microscope images of the large area emitter without (a) and with (b) hexagonal lens array

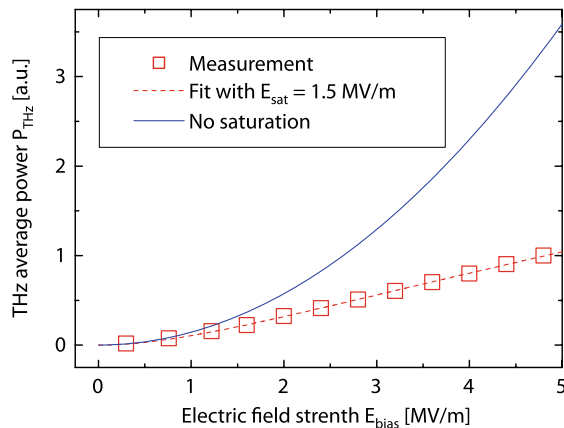


**Fig. 2** Influence of the saturation electric field strength on the generated THz average power. Optical excitation  $P_{\text{opt}} = 200$  mW

which ensures only constructive superposition of the generated THz waves. In this paper we present a further improved large-aperture emitter with an increased active area of about  $1 \times 1 \text{ mm}^2$  capable to deliver up to one order of magnitude higher THz emission in comparison to our former presented device [2].

## 2 Experiment and results

The investigated emitter structure is shown in Fig. 1. It consists of two finger electrodes on LT GaAs which are attached to a hexagonal microlens array. The finger electrodes (Ti/Pt/Au) have electrode widths of  $8 \mu\text{m}$  and gaps of  $5 \mu\text{m}$ . The microlenses made of fused silica have diameters of  $27 \mu\text{m}$  and a pitch of  $30 \mu\text{m}$ , which results in an overall hexagonal packaging density of 73.4 % (see Fig. 1b). A more detailed description of the fabrication process can be found in [2]. In our experiments, we used a common THz-time-domain system driven by a Ti:Sapphire laser with 150-fs pulses at a repetition rate of 80 MHz and a maximum average power of about 3 W (Spectra-Physics, Mai-Tai). In

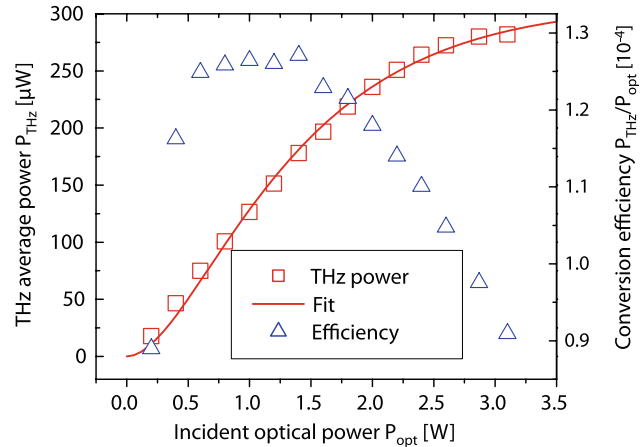


**Fig. 3** Measured THz average power and corresponding IR-to-THz conversion efficiency for the large-area microlens emitter. The corresponding fitting parameters are  $C/A^2 \approx 5 \times 10^{-17} \text{ m}^2/(\text{V}^2 \text{W})$ ,  $E_{\text{sat}} \approx 1.5 \text{ MV/m}$  and  $P_{\text{sat}} \approx 1 \text{ W}$

order to accelerate the generated charge carriers, we connected the electrodes to a 30-kHz/25-V square-wave voltage generator. The emitted THz waves were collected and directed by two off-axis parabolic mirrors onto a LT GaAs antenna with a gap of  $6 \mu\text{m}$  for phase-sensitive measurements. In addition, a pyroelectric detector was applied to measure the emitted THz average power. In [2] we derived the following mathematical expression for the THz output power  $P_{\text{THz}}$  depending on the absorbed optical power  $P_{\text{opt}}$  and applied electric field strength  $E_{\text{bias}}$ :

$$P_{\text{THz}} = \frac{CE_{\text{bias}}}{A^2} \cdot E_{\text{sat}} \left(1 - e^{-E_{\text{bias}}/E_{\text{sat}}}\right) \times P_{\text{sat}}^2 \left(1 - e^{-P_{\text{opt}}/P_{\text{sat}}}\right)^2. \quad (1)$$

This expression includes saturation effects which, on the one hand, depend on the absorbed optical intensity, i.e., screening effects, and, on the other hand, have their origin in the existence of a natural barrier for the maximum achievable electron acceleration which is defined by the saturation electric field strength  $E_{\text{sat}}$  [11]. A more detailed explanation of (1) can be found in [2]. In order to obtain  $E_{\text{sat}}$ , we measured the THz average power depending on the applied electric field strength while the incident pump power was kept constant. The experimental results are given in Fig. 2. The solid curve shows the calculated behavior for the absence of this saturation effect in order to illustrate the impact on the THz output.

Figure 3 shows the measured THz average power and corresponding conversion efficiency for increasing optical pumping. The applied acceleration field strength was about 5 MV/m. At around 0.5 W to 1.5 W pumping, significant saturation occurs, which results in a stagnating conversion efficiency at about  $1.3 \times 10^{-4}$ . At further increased pumping, the efficiency drops rapidly. This behavior can be at-

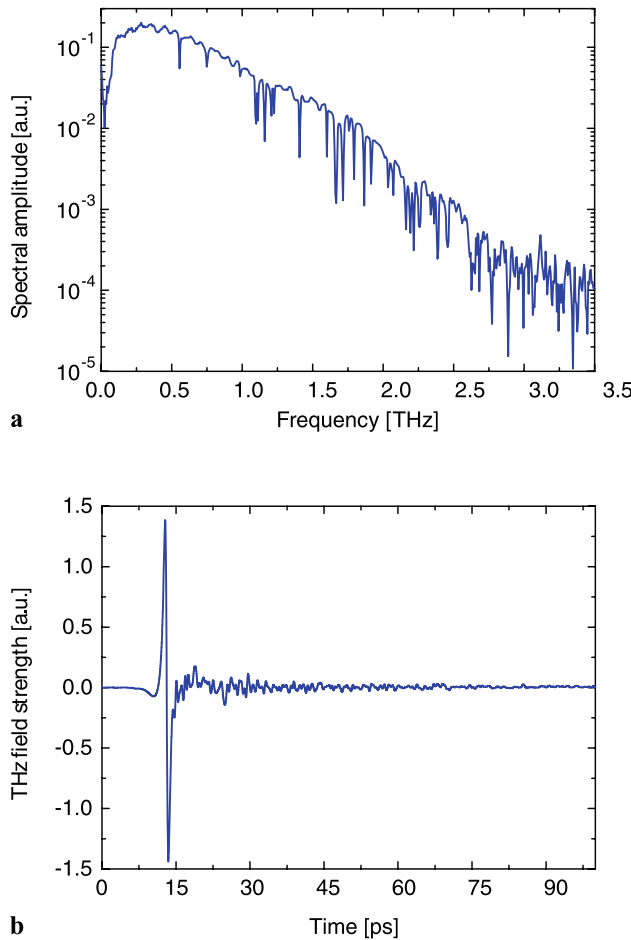


**Fig. 4** Time-domain THz field scan and corresponding THz spectrum at an applied electric field strength of 5 MV/m and an optical excitation of about 3 W. The sharp spectral lines are due to the water resonances caused by the water molecules in air

tributed to bleaching and electric field screening, which becomes increasingly relevant at higher photogenerated charge carrier densities [12, 13]. The corresponding optical saturation power  $P_{\text{sat}}$  was estimated to be around 1 W. Consequently, for higher pumping levels above 1 W, the emitter structure should be enlarged in order to keep the conversion efficiency high.

The THz electric field strength and corresponding spectral amplitude are shown for 3 W optical excitation in Fig. 4. Since we did not purge the THz path with nitrogen, absorption lines appear based on the content of water molecules in air.

### 3 Conclusion

In conclusion, we demonstrated the scaling potential of our previously presented microlens emitter [2]. The investigated

$1 \times 1 \text{ mm}^2$  finger electrode structure on LT GaAs delivers up to  $280 \mu\text{W}$  THz average power and a maximum conversion efficiency of about  $1.3 \times 10^{-4}$ . These results belong to the highest values ever reported using high-repetition rate lasers for THz excitation. Here, in contrast to typical large-aperture emitters where the center wavelengths are shifted to lower frequencies, finger electrodes in combination with microlenses guarantee high acceleration field strength and a broad THz spectrum even at illuminated areas above the  $\text{mm}^2$  range. For higher available optical power, the active area should be increased in order to preserve best conversion efficiencies. However, this requires a careful design of the antenna structure to minimize the dark current. Moreover, innovative cooling concepts have to be applied to overcome thermal limitations.

**Acknowledgements** We would like to acknowledge financial support from the Freistaat Thüringen (Grant No. 2006VF0020), the Bundesministerium für Wirtschaft und Technologie (Grant No. IW080064), and the European Fund for Regional Development (EFRE).

### References

1. A. Dreyhaupt, S. Winnerl, T. Dekorsky, M. Helm, *Appl. Phys. Lett.* **86**, 121114 (2005)
2. G. Matthäus, S. Nolte, R. Hohmuth, M. Voitsch, W. Richter, B. Pradarutti, S. Riehemann, G. Notni, A. Tünnermann, *Appl. Phys. Lett.* **93**, 091110 (2008)
3. M. Theuer, D. Molter, K. Maki, C. Otani, J.A. L'huillier, R. Beigang, *Appl. Phys. Lett.* **93**, 041119 (2008)
4. G. Matthäus, B. Ortat, J. Limpert, S. Nolte, R. Hohmuth, M. Voitsch, W. Richter, B. Pradarutti, A. Tünnermann, *Appl. Phys. Lett.* **93**, 261105 (2008)
5. J.A. L'huillier, G. Torosyan, M. Theuer, Y. Avetisyan, R. Beigang, *Appl. Phys. B* **86**, 185 (2007)
6. J.A. L'huillier, G. Torosyan, M. Theuer, C. Rau, Y. Avetisyan, R. Beigang, *Appl. Phys. B* **86**, 197 (2007)
7. J. Darmo, T. Müller, G. Strasser, K. Unterrainer, T. Le, A. Stingl, G. Tempea, *Opt. Lett.* **27**, 1941 (2002)
8. G. Chang, C.J. Divin, J. Yang, M.A. Musheinish, S.L. Williamson, A. Galvanauskas, T.B. Norris, *Opt. Express* **15**, 16308 (2007)
9. B. Pradarutti, R. Müller, G. Matthäus, C. Brückner, S. Riehemann, G. Notni, S. Nolte, A. Tünnermann, *Opt. Express* **15**, 17652 (2007)
10. B. Pradarutti, R. Müller, W. Freese, G. Matthäus, S. Riehemann, G. Notni, S. Nolte, A. Tünnermann, *Opt. Express* **16**, 18443 (2008)
11. J. Singh, *Electronic and Optoelectronic Properties of Semiconductor Structures* (Cambridge University Press, Cambridge, 2003)
12. J.E. Pedersen, V.G. Lyssenko, J.M. Hvam, P. Uhd Jepsen, S.R. Keiding, *Appl. Phys. Lett.* **62**, 1265 (1993)
13. D.S. Kim, D.S. Citrin, *Appl. Phys. Lett.* **88**, 161117 (2006)